

## Effects of gradient interlayer on residual stress and cracking in TiN thin films<sup>①</sup>

QI Xuan(漆璿), LI Ge-yang(李戈扬),

SHI Xiao-rong(施晓荣), LÜ Xia(吕霞), LI Peng-xing(李鹏兴)

*School of Materials Science and Engineering, Shanghai Jiaotong University,  
Shanghai 200030, P. R. China*

**Abstract:** The influence of a gradient interlayer on the residual stress and cracking in TiN thin films was studied as a function of the thickness of gradient interlayer. Both X-ray in-situ tensile testing and grazing method were used to measure the residual stress in thin films. In TiN films, there exists a residual stress of 10 GPa, which can be remarkably decreased by a gradient interlayer between film and substrate. The cracking behavior of films after tension shows that the crack of film/substrate system begins at interface between film and substrate.

**Key words:** TiN thin film; residual stress; gradient interlayer.

**Document code:** A

### 1 INTRODUCTION

The residual stress in films has important influence on the properties of a film/substrate system<sup>[1]</sup>. Previous research<sup>[2]</sup> on TiC/Al revealed that the magnitude of residual compressive stress in TiC thin films is as great as 10 GPa, which decreases remarkably with the increase of the thickness of gradient interlayer between film and substrate. In order to further confirm this conclusion and explore the decrease mechanism of residual stress of the film/substrate system, two kinds of X-ray diffraction methods were used to measure the residual stress in TiN films (AISI 304 substrate) with a gradient interlayer between the TiN film and substrate. The cracking behavior of film after tension is observed by optical microscopy and SEM. According to the experimental results, a mechanism on the initiation and the development of cracks in the film/substrate system is presented and the effects of the gradient interlayer on the residual stress of the film/substrate and cracking are discussed.

### 2 EXPERIMENTAL

#### 2.1 Sample preparation

TiN/stainless steel (AISI 304) composite system was designed as linear gradient interlayer. The designed thicknesses of gradient layer ( $h_g$ ) were 0 (no gradient layer), 100 nm, 300 nm and 500 nm, respectively. The composition change in the gradient interlayer from substrate to coating side was designed that the stainless steel-content decreased from 100% to 0 and TiN-content increased from 0 to 100%. A 2  $\mu$ m thick TiN coating was deposited on the surface of the

gradient layer. AES profile analysis of gradient layers is shown in Fig.1. The gradient layer and TiN coating were prepared by ANCLVA SPC-350 multi-target magnetic sputtering system. One RF target was TiN and the other was stainless steel. The gradient layer can be deposited by two targets alternatively by rotating the substrate holder. The change of gradient layer composition can be achieved by modifying the power of TiN and stainless steel targets.

The substrate was AISI 304 stainless steel, which was polished with 1  $\mu$ m diamond paste and then cleaned ultrasonically in acetone. Before sputtering, the chamber was evacuated and then cleaned by 50 eV Ar<sup>+</sup> beam sputtering.  $p_{Ar} = 4 \times 10^{-1}$  Pa during depositing. The distance between target and substrate was 80 mm. The substrate holder was rotated at a speed of 20 r/min.

#### 2.2 Residual stress measuring method

The residual stress was measured by normal grazing method (GM)<sup>[3]</sup> and the X-ray tensile testing (XTT) method. The former has been described<sup>[2]</sup>. The latter is a method proposed by Noyan et al for thin films research<sup>[4]</sup>. We have designed a mini-tensile tester for adhesion and residual stress measurement of thin films on metallic substrates<sup>[5,6]</sup>. This method is given as that, a plate tensile specimen (as shown in Fig.2(a)) with a gradient interlayer and a TiN coating on one side is extended by a mini-tensile tester mounted on the X-ray diffractometer. At the same time, the lattice space  $d_{hkl}$  parallel to the surface of thin film was measured by XRD. When the film adheres to the substrate and the yielding and cracking in the film does not occur, the  $d_{hkl}$  parallel to the film surface decreases gradually associated with the

① **Foundation item:** Project 9590015 - 02 supported by the National Natural Science Foundation of China

**Received date:** Mar.30, 1999; **accepted date:** Aug.15, 1999

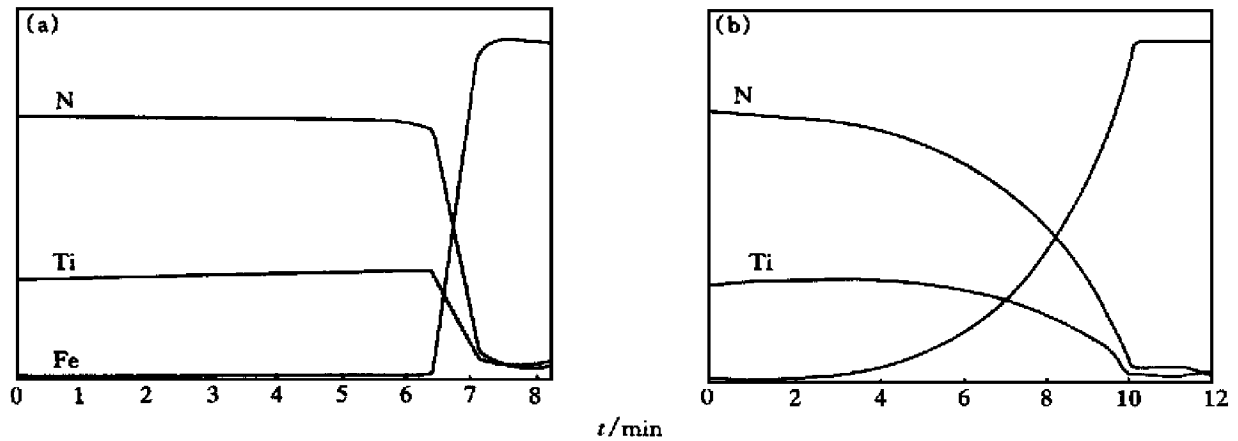


Fig. 1 AES profile analysis of gradient layers  
(a) — Without gradient layer; (b) — With 500 nm gradient layer

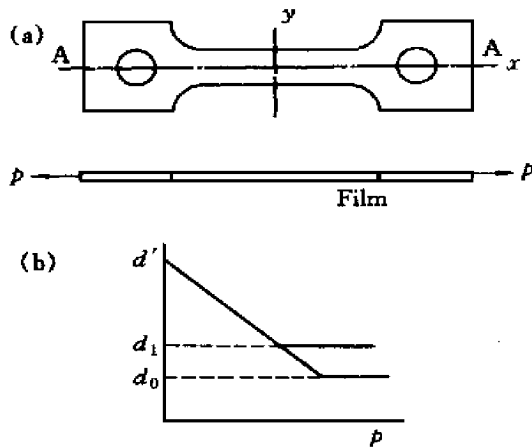


Fig. 2 Specimen for XTT (a) and schematic tensile curve (b)

relaxing of residual compressive stress in films; once the crack is initiated, the residual stress in film will be relaxed almost completely, the lattice space approached to  $d_0$  corresponding to the state of residual stress-free and afterwards it keeps constant as the specimen is extended continuously (see Fig. 2 (b)). Therefore, the residual stress ( $\sigma$ ) in films can be determined by measuring the difference between  $d'$  and  $d_0$ , i.e.  $\Delta d_{hkl}$ , where  $d'$  is the lattice space of  $hkl$  plane before extending. Assume that the residual stress in films is a planar stress condition<sup>[7]</sup>, then

$$\sigma_x = \sigma_y = \sigma \quad (1)$$

$$\text{so } \epsilon_z = -\frac{\nu}{E}(\sigma_x + \sigma_y) = -\frac{2\nu}{E}\sigma \quad (2)$$

$$\text{or } \epsilon_z = \frac{d' - d_0}{d_0} = \frac{\Delta d_{hkl}}{d_0} \quad (3)$$

$$\text{then } \sigma = -\frac{E}{2\nu} \cdot \frac{d' - d_0}{d_0} \quad (4)$$

where  $E$  and  $\nu$  are the elastic modulus and the Poisson ratio, respectively. If the residual stress  $\sigma_y$  is not relaxed, that is,  $\sigma_x = 0$ ,  $\sigma_y \neq 0$ , the lattice space  $d_1$  ( $d_1 \neq d_0$ ) after the crack being propagated can be de-

tected. In this condition,

$$\epsilon'_z = -\frac{\nu}{E}\sigma_y = -\frac{\nu}{E}\sigma \quad (5)$$

$$\text{and } \epsilon'_z = \frac{d_1 - d_0}{d_0} \quad (6)$$

$$\text{therefore } \sigma = -\frac{E}{\nu} \cdot \frac{d_1 - d_0}{d_0} \quad (7)$$

From Eqn.s (4) and (7)

$$d_0 = 2d_1 - d' \quad (8)$$

substitute Eqn. (8) into Eqn. (7)

$$\text{then } \sigma = \frac{E}{\nu} \cdot \frac{d' - d_1}{d' - 2d_1} \quad (9)$$

where  $E = 640$  GPa and  $\nu = 0.2$ <sup>[8]</sup>. Substitute  $d'$  and  $d$  into Eqn. (9),  $\sigma$  can be obtained.

After tension, the surface and cross-section (A—A) of specimens were observed by optical microscopy and SEM, respectively.

### 3 RESULTS AND DISCUSSION

#### 3.1 Residual stress in TiN thin films

The residual stress in TiN films measured by means of XTT and GM is listed in Table 1 and shown in Fig. 3. It is found that:

- 1) the values of residual stress in TiN films measured by different methods are close to 10 GPa, which are in agreement with those data of Elstner et al<sup>[9]</sup>;
- 2) the behavior of the decreased residual stress in TiN films by gradient interlayer is similar to that

Table 1 Data of residual stress measured in TiN films

No.	$h_g/\text{nm}$	$\sigma/\text{GPa}$	
		Grazing method	Tensile testing
0	0	-13.0	-14.2
1	100	-8.8	-12.8
3	300	-11.7	-10.9
5	500	-9.9	-8.4

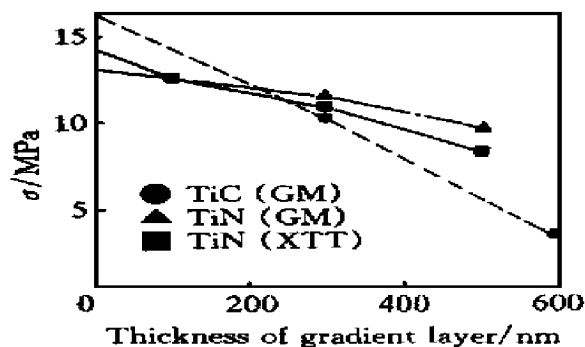


Fig.3 Effects of thickness of gradient layer on residual stress in films

observed in TiC/Al system<sup>[2]</sup>.

### 3.2 Relationship between cracking behavior and residual stress in films

It is easy to find that there are many cracks perpendicular to the extension direction and a few inclined cracks on film surface. The crack density decreases with the increase of interlayer thickness, as shown in Figs. 4 and 5.

Details can be found by SEM on cross-section of a specimen that the cross section morphology of cracks looks like a "droplet", whose maximum width is at the interface between film and substrate, and the global bottom of cracks is at the side of substrate.

The crack extends like a "wedge" towards the surface of TiN film (Fig. 6).

The above facts indicated that:

1) The cracking initiates at the film/substrate interface during tension. Since the extension of cracks in the side of substrate is impeded due to a good ductility of AISI 304, the tips of cracks become blunt and globular so that they fail to extend. However, in the side of brittle TiN film the cracks propagate and penetrate through the film. With the specimens being tensed continually, the residual compressive stress in the film surface appears to get smaller and smaller as the width of cracks increases, allowing the two sides of top gap of cracks to come into contact on the surface of the film. The cracks divide the film into some trapezoid parts, but the film still adheres with substrate so that the compressive stress is preserved in the films near substrate. The difference between the top and bottom width of the trapeze can be used to evaluate the values of compressive stress remaining in the films. The evaluated results agree with the measured values.

2) As mentioned above, the cracks in films result from the local plastic deformation of the substrate near the film. Therefore, the residual stress at interface region strongly affects the properties of film/substrate system. The gradient interlayer can delay the generation of the cracks in films and decrease the

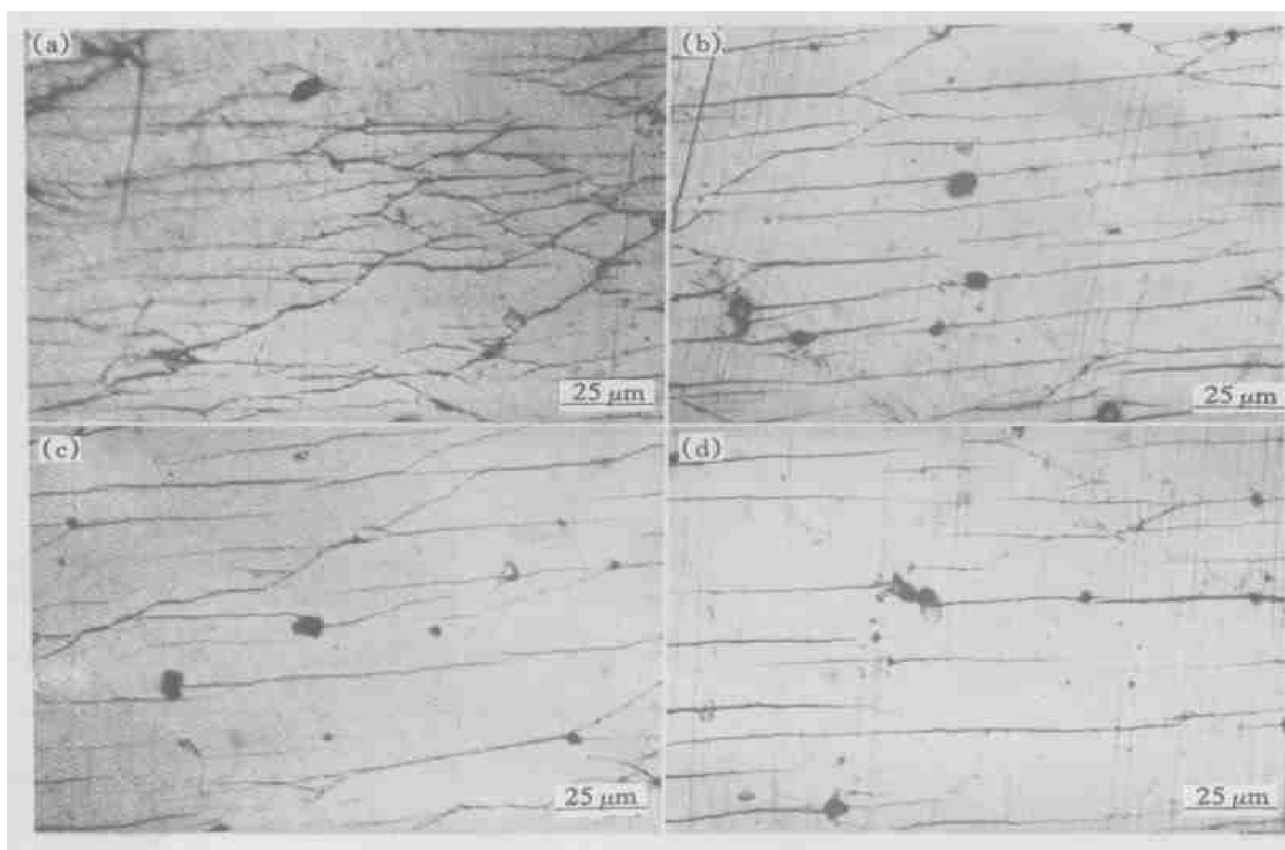


Fig.4 Micrographs of surface of specimens after extension  
(a)  $h_g = 0$ ; (b)  $h_g = 100$  nm; (c)  $h_g = 300$  nm; (d)  $h_g = 500$  nm

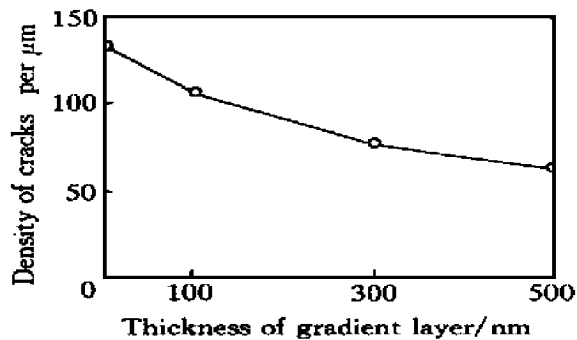


Fig. 5 Effect of interlayer thickness on density of cracks in films

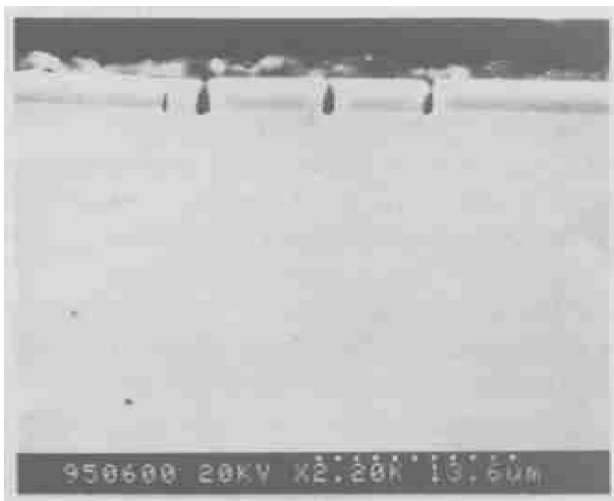


Fig. 6 SEM morphology of A—A section of extended specimen

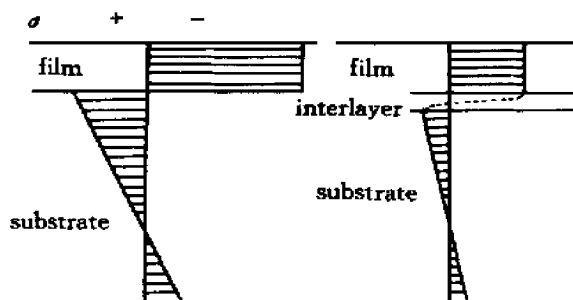


Fig. 7 Schematic representation of stress distribution across coating and substrate cross-section

number of cracks. Thornton and Hoffman<sup>[10]</sup> proposed a schematic diagram of stress distribution across film and substrate cross-section (Fig. 7). It is believed that the tensile stress must be maintained in the substrate near the film to balance the compressive stress in films. When the specimens are tensed, local yielding first occurs in the substrate region very near the film then the cracking occurs at the brittle TiN film adhering to the substrate, that is a cracking source. With an interlayer deposited between the substrate and the film, the intrinsic stress in film imposed in sputtering procedure will be relaxed easily through the plastic deformation in interlayer and substrate,

and then a few cracking sources form at the interface because of the lower residual tensile stress in substrate (as shown in Fig. 7).

#### 4 CONCLUSIONS

1) A residual compression stress (10 GPa) exists in hard brittle TiN films deposited by magnetron sputtering on the plastic substrate. The gradient interlayer between film and substrate can remarkably decrease the residual stress in the thin film.

2) The cracking sources in film/substrate system under tensile forces initiate at interface between film and substrate. The decrease of residual stress can remarkably delay the cracking in films and enhance the film failure resistance.

3) The X-ray tensile testing is an effective method to measure the residual stress in thin films and the measured results is close to those by using grazing method with parallel beam.

#### REFERENCES

- [1] Rickerby D S. Internal stress and adherence of titanium nitride coatings [J]. J Vac Sci Technol, 1986, A4(6): 2809 ~ 2814.
- [2] QI X, WANG Z M, LI G Y, et al. A study about the effect of gradient interlayer on the residual stress of TiC thin film by using X-ray grazing method [J]. Scripta Met Et Mater, 1994, 30(7): 881 ~ 884.
- [3] Goehner R P and Eatough M O. A study of grazing incidence configuration and their effect on X-ray diffraction data [J]. Powder Diffraction, 1992, 7(1): 2 ~ 5.
- [4] Noyan I C and Sheikh G. X-ray tensile testing of thin films [J]. J Mater Res, 1993, 8(4): 764 ~ 770.
- [5] LI G Y, CHEN C L, QI X, et al. An X-ray diffraction method for quantitative adhesion measurements of thin hard film on metallic substrates [A]. Proc of the 10th Inter Conf on Vac Metall [C], 1990, 2: 203 ~ 207.
- [6] LI G Y, QI X, SHI X R, et al. Influence of gradient layer on TiN coatings' internal stress [J]. Functional Materials, 1996, 27(6): 569 ~ 572.
- [7] Perry A J, Valvoda V and Rafaja D. X-ray residual stress measurement in TiN, ZrN and HfN films using the Seemann-Bohlin method [J]. Thin Solid Films, 1992, 214: 169 ~ 174.
- [8] Fillit R Y and Perry A J. Residual stress and X-ray elastic constants in highly textured physically vapor deposited coatings [J]. Surface and Coating Technol, 1988, 36: 647 ~ 659.
- [9] Elstner F, Ehrlich A, Giegengack H, et al. Structure and properties of titanium nitride thin films deposited at low temperatures using direct current magnetron sputtering [J]. J Vac Sci Technol, 1994, A12(2): 476 ~ 483.
- [10] Thornton J A and Hoffman D W. Thin Solid Films, 1989, 171(1-2): 5.

(Edited by HUANG Jin song)

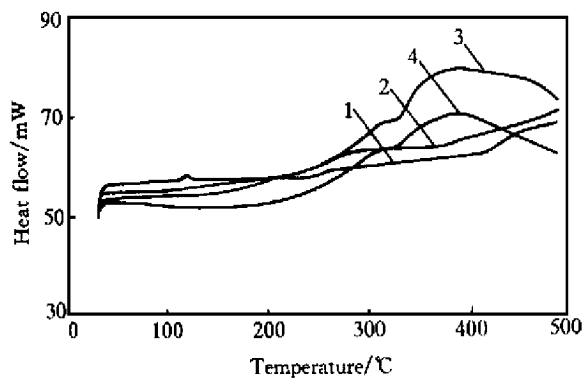


Fig. 4 DSC curves of mixed powders after different times of ball milling  
1—0 h; 2—4 h; 3—10 h; 4—10 h

tunity to diffuse to other side at a low temperature, stimulated by the crystal defects.

The most important interfacial reaction in Al-SiC system is  $\text{Al} + \text{SiC} \rightarrow \text{Al}_4\text{C}_3 + \text{Si}$ . Since  $\text{Al}_4\text{C}_3$  is a brittle phase and has poor anticorrosion property, this reaction is often regarded harmful<sup>[9]</sup>. There are two reasons for the low level of interface reaction in our high-energy ball milling experiment. First, this reaction need a temperature as high as  $650 \sim 700^\circ\text{C}$ <sup>[5, 10]</sup>, however, the experimental temperature was not high enough for the reaction. Second, the solubility of  $\text{Al}_4\text{C}_3$  in the Al matrix is quite small, in terms of the theory of chemical reaction balance, in order to produce more  $\text{Al}_4\text{C}_3$ , more Si should be removed or dissolved into the Al matrix. Since Al-30Si powders contain a large amount of Si, it is difficult for the reaction to proceed rightward. In other words, the reaction has been retarded due to both thermodynamics and kinetics.

As the hardness of  $\text{SiC}_p$  is far higher than that of Al-30Si alloy powder, after ball milling for a long time, some of SiC particles were pressed into alloy powder, which brings two advantages to MMC fabrication process. First, it can ease the wearability of the mould and improve shaping ability of the mixed powders. Second, since the wettability between the same type of materials is better than that of different one, it can promote sintering process to attain stronger bonding. In fact, some researchers have used high-energy ball milling to fabricate Al/ $\text{SiC}_p$  composites<sup>[11]</sup>. Considering the equipment condition and the cost, high-energy ball milling can serve as an effective reinforcement pre-treatment method in the fabrication of MMC.

## 5 CONCLUSIONS

1) Through high-energy ball milling, both Al-

30Si alloy powders and their microstructure are obviously refined.

2) After high-energy ball milling, close-contacted interface is formed between the alloy powders and  $\text{SiC}_p$  without interfacial reaction. No reaction but relaxation of the powder can be detected by DSC.

## ACKNOWLEDGEMENT

Most experimental work of this paper was finished in Metal Physics Institute, Technical University Berlin, German. The authors would like to express heartfelt thanks to professor H.J. Fecht for his help.

## REFERENCES

- [1] Zhou J, Duszczak J and Korevaar B M. Microstructural features and final mechanical properties of the iron modified Al-20Si-3Cu-1Mg alloy processed from atomised powder [J]. *J. Mater. Sci.*, 1991, 26: 3041.
- [2] Ward P J and Atkinson H V. Semi-solid processing of novel MMCs based on hypereutectic aluminium-silicon alloys [J]. *Acta Mater.*, 1996, 44(5): 1717.
- [3] Gupta M and Lavernia E J. Effect of processing on the microstructure variation and heat-treatment response of a hypereutectic Al-Si alloy [J]. *J. Mater. Process. Technol.*, 1995, 54: 261.
- [4] Loyd D J. Particle reinforced aluminium and magnesium matrix composites [J]. *Inter. Mater. Rev.*, 1994, 39: 1.
- [5] Wang W, Ajersch F and Lofvander J P A. Si phase nucleation on SiC particulate reinforcement hypereutectic Al-Si alloy matrix [J]. *Mater. Sci. Eng.*, 1994, A187: 65.
- [6] Lindroos V K and Talvite M J. Recent advances in metal matrix composites [J]. *J. Mater. Process. Tech.*, 1995, 53: 273.
- [7] Wang B, Janowski G M and Patterson B R. SiC particle cracking in powder metallurgy processed aluminium matrix composite materials [J]. *Metall. Mater. Trans.*, 1995, 26A: 2457.
- [8] LI Yuan-yuan, ZHANG Da-tong, XIA Wei, et al. Properties of a high silicon aluminium alloy powder prepared by high pressure water atomization [J]. *Acta Metall. Sin.*, (in Chinese), 1998, 34: 95.
- [9] Ferro A C and Derby B. Wetting behavior in the Al-Si/SiC system: interface reaction and solubility effects [J]. *Acta Metall. Mater.*, 1995, 43: 3601.
- [10] Viala J C, Fortier P and Boutier J. Stable and metastable phase equilibria in the chemical interaction between aluminium and silicon carbides [J]. *J. Mater. Sci.*, 1990, 25: 1842.
- [11] Nobel B, Trowsdale A J and Harris S J. Low temperature interface reaction in aluminium-silicon carbide particulate composites produced by mechanical alloying [J]. *J. Mater. Sci.*, 1997, 32: 5969.

(Edited by LONG Huai-zhong)